

Measurement of the nuclear reaction  ${}^7\text{Li}({}^3\text{He}, p_0){}^9\text{Be}$  at low energiesJ. Yan,<sup>1</sup> F. E. Cecil,<sup>1</sup> U. Greife,<sup>1</sup> C. C. Jewett,<sup>1</sup> R. J. Peterson,<sup>2</sup> and R. A. Ristenin<sup>2</sup><sup>1</sup>Department of Physics, Colorado School of Mines, Golden, Colorado 80401<sup>2</sup>Department of Physics, University of Colorado, Boulder, Colorado 80302

(Received 7 November 2001; published 1 April 2002)

The nuclear reaction  ${}^7\text{Li}({}^3\text{He}, p_0){}^9\text{Be}$  was measured at effective center-of-mass energies of  $E=106.3$  and  $E=112.8$  keV with the 180-kV Cockcroft-Walton accelerator at the Colorado School of Mines. As this reaction is a possible contributor to inhomogeneous big bang nucleosynthesis, all published data were compiled and used, together with our measurement, in a calculation of the thermonuclear reaction rate for temperatures up to  $10^9$  K.

DOI: 10.1103/PhysRevC.65.048801

PACS number(s): 26.35.+c, 21.10.Jx, 25.55.-e

Recent precision measurements in cosmology, i.e., the COBE, BOOMERANG, or MAXIMA-1 experiments [1–5], determined parameters relevant to the birth of our universe with a level of precision comparable to the accuracy of the predictions derived from big bang nucleosynthesis. However, a comparison reveals discrepancies, the most striking one being the derived baryon density  $\Omega_B$ . Here the standard model of big bang nucleosynthesis [6] uses an upper limit of  $\Omega_B=0.02$ , while the BOOMERANG data suggest an  $\Omega_B$  of 0.05 and MAXIMA-1 a value of 0.07. Inhomogeneous models of big bang nucleosynthesis, however, do allow higher values of  $\Omega_B$ , up to 0.10, that would include the above measurements [6–8]. One difference between the standard model and inhomogeneous models is that the latter consider a wider reaction network, which can increase the production of  ${}^7\text{Li}$  as well as the abundances of heavier nuclei. A puzzle piece in this reaction network, the nuclear reaction  ${}^7\text{Li}({}^3\text{He}, p_0){}^9\text{Be}$  processes some  ${}^7\text{Li}$  to  ${}^9\text{Be}$ , thus bridging the mass-8 gap. In this reaction only the proton emission to the ground state leads to  ${}^9\text{Be}$  production as all the excited states in  ${}^9\text{Be}$  are unbound to  $2\alpha+n$  decay.

The most recent experimental determination of  ${}^7\text{Li}({}^3\text{He}, p_0){}^9\text{Be}$  dates back to 1990, where Rath *et al.* [9] published a measurement ranging in energy from  $E_{\text{c.m.}}=0.5$  to 2.0 MeV. Yamamoto, Kajino, and Kubo used their results [10] in a theoretical description to extrapolate into the Gamow energy region for big bang nucleosynthesis around  $E_{\text{c.m.}}=400$  keV, and to extract reaction parameters for a description of the competing reaction  ${}^7\text{Li}(t, n){}^9\text{Be}$ , which according to present estimates of big bang nucleosynthesis dominates  ${}^9\text{Be}$  production. In order to check the extrapolation, we performed a new measurement of the  ${}^7\text{Li}({}^3\text{He}, p_0){}^9\text{Be}$  cross section at energies below the center of the Gamow peak.

The measurements were carried out using the low energy, high current accelerator at the Colorado School of Mines. The targets consisted of thick foils of analytically pure lithium metal of natural isotopic abundances ( ${}^7\text{Li}=93.5\%$ ). In order to minimize oxidation of the target surfaces, the lithium was stored in mineral oil then polished in an Ar atmosphere, and transferred under vacuum to a small scattering chamber. Reaction products were detected with a standard two-detector silicon surface barrier detector telescope. Reaction product energies from each detector were stored on

an event by event basis allowing an *ex-post-facto* construction of a two-dimension (2D) plot of total energy vs energy loss in the front detector. Both detectors had a surface area of  $300\text{ mm}^2$ . The front  $\Delta E$  detector had a thickness of  $150\text{ }\mu\text{m}$  and the back  $E'$  detector had a thickness of  $500\text{ }\mu\text{m}$ . Because of the expected small yields, the solid angle of the telescope was optimized by placing the detectors as close as possible to the target. The center of the front of the  $\Delta E$  detector was 27 mm from the center of the target and at an angle of  $105^\circ$  from the forward beam direction. The projectiles were produced out of 99.8% enriched  ${}^3\text{He}$  gas, resulting in a magnetically analyzed  ${}^3\text{He}^+$  with a very small fraction ( $\sim 10^{-7}$  as determined by observation of proton and deuteron induced reactions) of singly ionized molecular ( ${}^1\text{H}-{}^2\text{H}$ )<sup>+</sup> which resulted from previous uses of hydrogen and deuterium beams and which had virtually the same magnetic rigidity as the  ${}^3\text{He}^+$ . This small component of protons and deuterons did produce significant yields of spurious reaction products from the  ${}^6\text{Li}(p, \alpha){}^3\text{He}$ ,  ${}^7\text{Li}(p, \alpha){}^4\text{He}$ ,  ${}^7\text{Li}(d, \alpha){}^5\text{He}$ , and  ${}^3\text{He}(d, p){}^4\text{He}$  reactions (where the target  ${}^3\text{He}$  in this last reaction results from the impacted beam ions in the Li target).

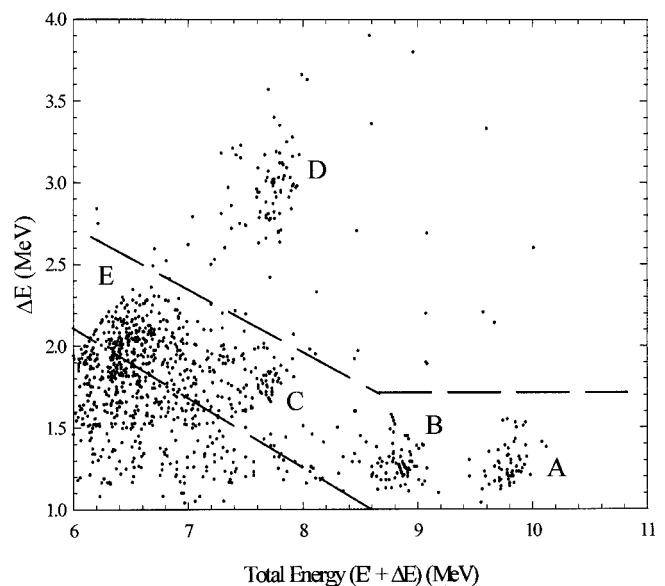


FIG. 1. The  $\Delta E$ - $E$  spectrum measured at a  ${}^3\text{He}$  bombarding energy of 170 keV.

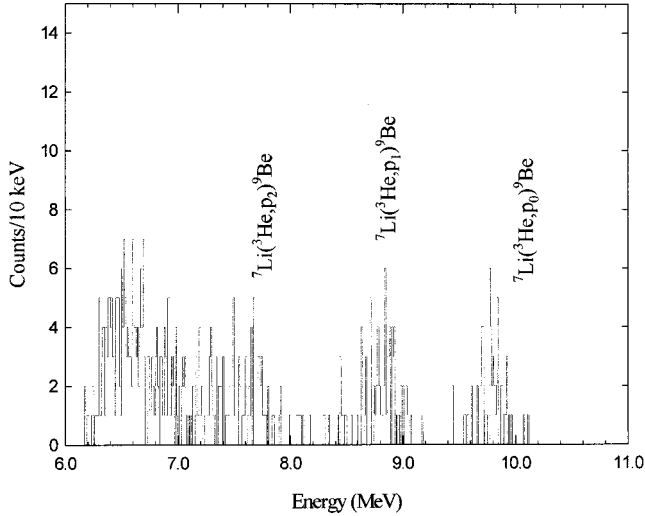


FIG. 2. The proton energy spectrum projected out of the region in Fig. 1 between the dashed lines.

All of these reaction products could be distinguished from the proton groups from the  ${}^7\text{Li}({}^3\text{He}, p){}^9\text{Be}$  reaction by use of the 2D  $\Delta E$  vs  $E$  plot. An example of a 2D plot measured at a  ${}^3\text{He}$  laboratory bombarding energy of 170 keV is shown in Fig. 1. The groups A, B, and C correspond to the reactions  ${}^7\text{Li}({}^3\text{He}, p_0){}^9\text{Be}$ ,  ${}^7\text{Li}({}^3\text{He}, p_1){}^9\text{Be}$ , and  ${}^7\text{Li}({}^3\text{He}, p_2){}^9\text{Be}$ . Group D is due to the reaction  ${}^7\text{Li}({}^3\text{He}, d_1){}^8\text{Be}$ . There was no evidence for the  $({}^3\text{He}, d)$  reaction to the  ${}^8\text{Be}$  ground state. Also missing is any evidence of the reaction  ${}^3\text{He}({}^3\text{He}, 2p)\alpha$  which, being a three-body final-state reaction, will produce a continuum of proton energies up to 10.4 MeV and would be manifest as a continuous distribution of points between groups A, B, and C. The broad collection of protons at group E results from the 14.9 MeV protons from the  ${}^3\text{He}(d, p){}^4\text{He}$  reaction. These protons do not stop in the back detector and lose about 6.5 MeV in the combined two-detector telescope.

The proton energy spectrum generated by projecting out the counts between the two dashed lines in Fig. 1 is shown in Fig. 2. The yield of a given reaction product can either be derived from the peak in Fig. 2 or the corresponding group in Fig. 1. Since the targets were thick compared to the range of the  ${}^3\text{He}$  beam ions, the yields represent an integrated yield as the beam ions slow down in the target. The methodology we used to extract the  $S$  factors effective energies was identical to that which we used in our recent study of deuteron in-

TABLE I. Results from measurements of  ${}^7\text{Li}({}^3\text{He}, p_0){}^9\text{Be}$  reaction.

$E_{\text{lab}}$ (keV) <sup>a</sup>	Charge (C)	$E_{\text{c.m.}}$ (keV) <sup>b</sup>	$E_{\text{eff/c.m.}}$ (keV) <sup>c</sup>	$S$ (MeV b)
160	1.285	111.9	106.3	$6.0 \pm 0.8$
170	0.578	118.9	112.8	$6.5 \pm 1.0$

<sup>a</sup> ${}^3\text{He}$  laboratory bombarding energy.

<sup>b</sup>Total energy of the  ${}^3\text{He}$  and  ${}^7\text{Li}$  in the center of mass.

<sup>c</sup>Total effective reaction energy of the  ${}^3\text{He}$  and  ${}^7\text{Li}$  in the center of mass.

TABLE II. Compiled astrophysical  $S$ -factor information of  ${}^7\text{Li}({}^3\text{He}, p_0){}^9\text{Be}$ .

$E_{\text{c.m.}}$ (MeV)	$S(E_{\text{c.m.}})$ (MeV b)
0.1063 <sup>a</sup>	$6.0 \pm 0.8$
0.1128 <sup>a</sup>	$6.5 \pm 1.0$
0.416 <sup>b</sup>	$16.2 \pm 1.7$
0.489 <sup>b</sup>	$19.9 \pm 2.1$
0.511 <sup>b</sup>	$23.2 \pm 2.8$
0.519 <sup>b</sup>	$24.5 \pm 2.9$
0.550 <sup>b</sup>	$29.9 \pm 3.3$
0.590 <sup>b</sup>	$42.0 \pm 4.5$
0.627 <sup>b</sup>	$41.5 \pm 3.5$
0.677 <sup>b</sup>	$39.1 \pm 4.0$
0.698 <sup>b</sup>	$38.7 \pm 3.9$
0.746 <sup>b</sup>	$34.6 \pm 3.1$
0.782 <sup>b</sup>	$29.9 \pm 2.4$
0.853 <sup>b</sup>	$28.5 \pm 2.8$
0.890 <sup>b</sup>	$25.5 \pm 2.2$
0.948 <sup>b</sup>	$21.3 \pm 1.2$
0.991 <sup>b</sup>	$19.0 \pm 1.3$
1.028 <sup>b</sup>	$17.9 \pm 0.9$
1.065 <sup>b</sup>	$15.8 \pm 1.2$
1.088 <sup>b</sup>	$15.5 \pm 0.9$
1.153 <sup>b</sup>	$13.1 \pm 1.0$
1.205 <sup>b</sup>	$13.4 \pm 0.7$
1.25 <sup>b</sup>	$12.8 \pm 0.7$
1.315 <sup>b</sup>	$12.8 \pm 0.7$
1.336 <sup>b</sup>	$11.4 \pm 0.6$
1.371 <sup>b</sup>	$11.3 \pm 0.7$
1.446 <sup>b</sup>	$9.1 \pm 0.4$
1.552 <sup>b</sup>	$10.6 \pm 0.5$
1.666 <sup>b</sup>	$9.1 \pm 0.5$
1.737 <sup>b</sup>	$8.0 \pm 0.4$
1.815 <sup>b</sup>	$7.4 \pm 0.4$
2.1 <sup>c</sup>	$9.6 \pm 1.0$
2.24 <sup>d</sup>	$9.0 \pm 0.9$
3.15 <sup>d</sup>	$3.8 \pm 0.5$
6.99 <sup>e</sup>	$1.1 \pm 0.2$

<sup>a</sup>This work.

<sup>b</sup>Reference [9].

<sup>c</sup>Reference [12].

<sup>d</sup>Reference [13].

<sup>e</sup>Reference [14].

duced reactions on  ${}^9\text{Be}$ ,  ${}^{10}\text{B}$ , and  ${}^{11}\text{B}$  [15] and will not be reproduced here. In addition we assumed isotropic angular distributions for a solid angle coverage of 0.36 sr. The results, together with the accumulated charge at each measurement, at the two laboratory bombarding energies of 160 and 170 keV are given in Table I.

This experiment provided two data points as shown in Table I. Since the results are approximately 40% lower than the published extrapolation of Rath *et al.* [9] and Yamamoto, Kajino, and Kubo [10], we decided to provide a new  $S$ -factor description. Specifically, our data hinted at a significantly

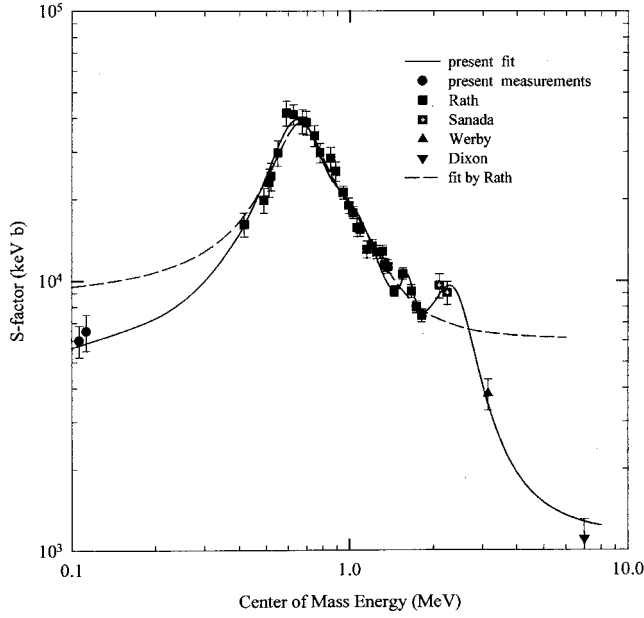


FIG. 3. A summary of all measurements of the astrophysical  $S$  factor of the  ${}^7\text{Li}({}^3\text{He},p_0){}^9\text{Be}(\text{g.s.})$ .

TABLE III. Parameters for the  $S$ -factor fit.

Resonance	$E_i$ (MeV)	$\Gamma_i$ (MeV)	$C_i$ (MeV <sup>3</sup> b)
1	0.643	0.34	$0.980 \pm 0.039$
2	1.01	0.6	$1.007 \pm 0.043$
3	1.61	0.21	$0.041 \pm 0.006$
4	2.31	1.0	$1.859 \pm 0.159$
(5) direct			$1.137 \pm 0.189^{\text{a}}$

<sup>a</sup>[MeV b].

lower direct-process contribution than the previous publications assumed.

We incorporated our data with all other published information to derive an  $S$ -factor description, which can be used for the calculation of thermonuclear reaction rates. Most of the data [9,12–14] were not available in tabulated form, so we had to read them out of the published figures. We also had to estimate some of the assigned errors. We provide Table II to sum up the  $S$ -factor information we used. We employed this and our data in a Breit-Wigner fit using the known resonances [9,11] and a direct reaction component (which we assumed to be constant for simplification purposes) for a description of the  $S$  factor,

TABLE IV. Reaction rate,  $\langle\sigma v\rangle$ , for  ${}^7\text{Li}({}^3\text{He},p_0){}^9\text{Be}$ .

$T_9$ (K)	$\langle\sigma v\rangle$ (cm <sup>3</sup> /mol/s) <sup>a</sup>	$\langle\sigma v\rangle$ (cm <sup>3</sup> /mol/s) <sup>b</sup>
0.1	$4.51 \times 10^{-6}$	$7.39 \times 10^{-6}$
0.2	0.010	0.015
0.3	0.48	0.65
0.4	5.86	7.15
0.5	37.0	41.8
0.6	153	164
0.7	474	490
0.8	1174	1192
0.9	2470	2482
1.0	4580	4580

<sup>a</sup>Present work.

<sup>b</sup>Reference [9].

$$S(E) = C_1 / [(E - E_1)^2 + (\Gamma_1/2)^2] + C_2 / [(E - E_2)^2 + (\Gamma_2/2)^2] + C_3 / [(E - E_3)^2 + (\Gamma_3/2)^2] + C_4 / [(E - E_4)^2 + (\Gamma_4/2)^2] + C_5.$$

The data, our fit, and the fit from Ref. [9] are depicted in Fig. 3; the fit parameters are given in Table III. Using the following equation, we then calculated by numerical integration the thermonuclear reaction rate for this reaction:

$$N_A(\sigma v) = (8/\pi\mu)^{1/2} N_A / (kT)^{3/2} \int S(E) \times \exp(-E/kT - bE^{-1/2}) dE.$$

The results of this calculation are summarized in Table IV where they are compared to the reaction rates calculated by Rath *et al.* [9]. It should be noted that the present reaction rates are about 60% of those presented in Ref. [9] at the lowest temperatures.

The nuclear reaction  ${}^7\text{Li}({}^3\text{He},p_0){}^9\text{Be}$  was measured at very low energies below the center of the Gamow peak region in big-bang nucleosynthesis. Using all other available information, we derived an  $S$ -factor description for the relevant energy range. Because the direct reaction component appears to have been overestimated by about a factor of 5 in previous work, the thermonuclear reaction rate calculated in this work is lower than previously published values.

This work was performed under a grant from the U.S. Department of Energy (Grant No. DE-FG03-93ER40789).

[1] G. Smoot *et al.*, *Astrophys. J. Lett.* **396**, L1 (1992).  
 [2] P. Bernadis *et al.*, *Nature (London)* **404**, 955 (2000).  
 [3] A. Lange *et al.*, *Phys. Rev. D* **63**, 042001 (2001).  
 [4] S. Hanany *et al.*, *Astrophys. J. Lett.* **545**, L5 (2000).  
 [5] A. Balbi *et al.*, *Astrophys. J. Lett.* **545**, L1 (2000).  
 [6] R. N. Boyd, *Nucl. Phys.* **A693**, 249 (2001).  
 [7] G. Steigman, N. Hata, and J. F. Felten, *Astrophys. J.* **510**, 564 (1999).  
 [8] B. Fields (unpublished).

[9] D. P. Rath, R. N. Boyd, H. J. Hausman, M. S. Islam, and G. W. Kolnicki, *Nucl. Phys.* **A515**, 338 (1990).  
 [10] Y. Yamamoto, T. Kajino, and K.-I. Kubo, *Phys. Rev. C* **47**, 846 (1993).  
 [11] F. Ajzenberg-Selove, *Nucl. Phys.* **A413**, 1 (1984).  
 [12] J. Sanada *et al.*, *J. Phys. Soc. Jpn.* **26**, 853 (1969).  
 [13] M. F. Werby and S. Edwards, *Nucl. Phys.* **A213**, 294 (1973).  
 [14] R. L. Dixon and R. D. Edge, *Nucl. Phys.* **A156**, 33 (1970).  
 [15] Jinsheng Yan *et al.*, *Phys. Rev. C* **55**, 1890 (1997).